Preparation, characterization and luminescence properties of pyrochlore $La_2Zr_2O_7:Eu^{3+}$ nanofibers by electrospinning

RENYUAN LIU, XIANGTING DONG*, JINXIAN WANG, WENSHENG YU, GUIXIA LIU
Key Laboratory of Applied Chemistry and Nanotechnology at Universities of Jilin Province, Changchun University of Science and Technology, Changchun 130022, P. R. of China

One-dimensional Eu^{3+}-doped $La_2Zr_2O_7$ nanofibers were fabricated by a simple and effective electrospinning combined with sol-gel process. The structural properties were characterized by thermogravimetric and differential thermal analysis(TG-DTA), x-ray diffraction(XRD), field emission scanning electron microscope(FESEM), and energy-dispersive x-ray spectroscopy(EDS). XRD analysis indicates that $La_2Zr_2O_7:Eu^{3+}$ nanofibers are pyrochlore in structure with space group Fd-3m. FESEM analysis indicates the surface of $La_2Zr_2O_7:Eu^{3+}$ nanofibers is coarse, the average diameter is *ca.* 190nm. The photoluminescent(PL) properties of the $La_2Zr_2O_7:Eu^{3+}$ nanofibers were also studied. It is observed that the charge-transfer excitation peak of Eu^{3+}-O^{2-} is 279 nm, absorption peak of $La_2Zr_2O_7$ matrix is 228 nm. Under excitation of 279nm, $La_2Zr_2O_7$:5%Eu^{3+} nanofibers emit the main emission at 587 nm, corresponding to $^5D_0$-$^7F_1$ transition of Eu^{3+}; under excitation of 228 nm, $La_2Zr_2O_7$:5%Eu^{3+} nanofibers emit the main emission at 580 nm, corresponding to $^5D_0$-$^7F_0$ transition of Eu^{3+}. Possible formation mechanism of $La_2Zr_2O_7:Eu^{3+}$ nanofiber was proposed.

(Received September 5, 2012; accepted May 15, 2014)

Keywords: Electrospinning, $La_2Zr_2O_7:Eu^{3+}$, Nanofiber, Luminescence properties

1. Introduction

One-dimensional(1D) and Quasi-one-dimensional(Q-1D) nanostructures, such as nanowires, nanofibers, nanorods, nanobelts, and nanotubes, have attracted great research interests, due to its special electronic properties, such as the increase of surface to volume ratio and quantum confinement effects [1-3]. They not only can play a crucial role in important future optoelectronic devices, data storage, and biochemical and chemical sensors but also can be used to enrich our understanding of basic quantum mechanics. Up to now, various techniques have been explored to prepare 1D and Q-1D nanomaterials, such as laser ablation, vapor-phase approach, template, and other methods [4-6]. Compared with these methods, electrospinning provides a promising, straightforward and convenient way to fabricate 1D and Q-1D nanomaterials with the characteristics of easy control and low cost [7-9].

$La_2Zr_2O_7$ with a pyrochlore structure are of great interest in recent years for their high thermal stability, low thermal conductivity [10], relatively high interstitial oxygen ion incorporation and possible high ionic conductivities [11]. It has been reported as a solid electrolyte in high-temperature fuel cell, thermal barrier coatings, oxidation catalysts and host materials for luminescence centers. $La_2Zr_2O_7$ has been prepared by various techniques such as ceramic, sol-gel [12], co-precipitation [13], inorganic sol-gel [14], hydrothermal, hydrazine methods [15] and the solid-state decomposition of metal nitrate–urea mixtures [16]. Wang [17] investigated temperature dependent photoluminescence of nanocrystalline $Y_2Zr_2O_7:Eu^{3+}$, However, the investigation on the photoluminescent(PL) property of $La_2Zr_2O_7:Eu^{3+}$ 1D nanomaterials is still lacking.

Here, we report the preparation of Eu^{3+} doped $La_2Zr_2O_7$ phosphors via a simple and effective electrospinning method. We also investigate the structure, morphology, and PL properties of the resulting samples in detail and some meaningful results were obtained.

2. Experimental sections

2.1 Chemicals

Polyvinyl pyrrolidone (PVP, K-90) and N, N-dimethyl formamide (DMF) were purchased from Tianjin Tiantai Fine Chemical Reagents Co. Ltd. and HNO_3 (A.R.) was purchased from Beijing Chemical Company. Eu_2O_3, $La(NO_3)_3{\cdot}6H_2O$ was purchased from Sinopharm Chemical Reagents Co. Ltd. Zirconium oxychloride octahydrate was bought from the Third

Chemical Reagents of Tianjin. $Eu(NO_3)_3$ was prepared by dissolving Eu_2O_3 in dilute nitric acid, then evaporated the water in the solutions by heating. 36wt% $ZrOCl_2$ was prepared by dissolving $ZrOCl_2{\cdot}8H_2O$ into deionized water. All chemicals were of analytical grade and directly used as received without further purification.

2.2 Preparation of samples

$La_2Zr_2O_7$:5 mol%Eu^{3+} nanofibers were prepared by a method of electronspinning combined with sol–gel process. 0.95 mmol $La(NO_3)_36H_2O$, 0.05 mmol $Eu(NO_3)_3$ and 0.9 g 36wt% $ZrOCl_2$ were dissolved in 11.4 g DMF, then 2.3 g PVP (15 wt%) was added. The solution was stirred for 8 h to form a homogeneous mixture sol for further electrospinning.

The electrospinning setup consists of three major components: a high voltage power supply, a spinneret(syringe), and a collector plate(a grounded conductor). The precursor sol was loaded into the syringe. In a typical electrospinning process, the precursor sol was ejected from the tip of the spinneret under the effect of high voltage that was applied between the spinneret and the collector to form an electrically charged jet of sol. The sol jet solidified with evaporation of solvent and formed a nonwoven mat on the collector [1].

The distance between the spinneret(a plastic needle) and collector(aluminum foil) was fixed at 20 cm and the high voltage supply was maintained at 16 kV. The room temperature is 20-24 °C and the relative humidity is 50-60 %. $[La(NO_3)_3+ZrOCl_2+Eu(NO_3)_3]$/PVP composite nanofibers would be fabricated. $La_2Zr_2O_7$:5 mol% Eu^{3+} nanofibers can be obtained when the relevant composite nanofibers were annealed in air at the desired temperature for 8h with the heating rate of 1 °C·min^{-1}. $La_2Zr_2O_7$ nanofibers were prepared by the similar procedure, by keeping the molar rate of La^{3+} to Zr^{4+} is 1:1.

2.3 Characterization methods

X-ray powder diffraction(XRD) measurements were carried out on a Dandong Y-2000 diffractometer using Cu Ka radiation with Ni filter(λ=0.15405nm), and the operation voltage and current were kept at 40kV and 20mA, respectively. Thermogravimetric and differential thermal analysis(TG-DTA) data were recorded with Pyris Diamond TG-DTA(PerkinElmer Thermal Analyzer) with the heating rate of 10 °C·min^{-1} in an air flow of 25 ml·min^{-1}. Morphology and composition of the samples were analyzed using a field emission scanning electron microscope(FESEM, XL-30, FEI Company) equipped with an energy-dispersive x-ray spectroscopy (EDS, JEOL JXA-840). The photoluminescence(PL) measurements were performed on a Hitachi F-7000 spectrophotometer equipped with a 150W xenon lamp as the excitation source.

3. Results and discussion

3.1 TG-DTA Analysis

Fig. 1 shows the thermal behavior of $[La(NO_3)_3+ZrOCl_2)]$/PVP composite nanofibers. The weight loss was involved in four stages in TG curve. The first weight loss is 12.2% in the range of 40 to 160ºC accompanied by a small endothermic peak near 70ºC in the DTA curve, which is caused by the loss of the surface absorbed water or the solvents DMF in the composite nanofibers. The second weight loss (59.9%) is between 160 and 326ºC accompanied by a sharp exothermic peaks near 320°C in the DTA curve because of the decomposition of the nitrate and PVP [18]. The third weight loss is 13.5% in the range from 326 to 446ºC. In the DTA curve, a small exothermic peak is located at 405ºC, which is attributed to the oxidation of carbon and carbon monoxide released by the decomposition of PVP [19]. The fourth weight loss (6.2%) accompanied by a small exothermic peak near 470ºC in the DTA curve is the result of the decomposition of $ZrOCl_2$ and residual organics. And above 900°C, the TG curve is unvaried, indicating that solvents, organic compounds, nitrate and $ZrOCl_2$ in the composite nanofibers volatilize completely. The total weight loss is 94.6%.

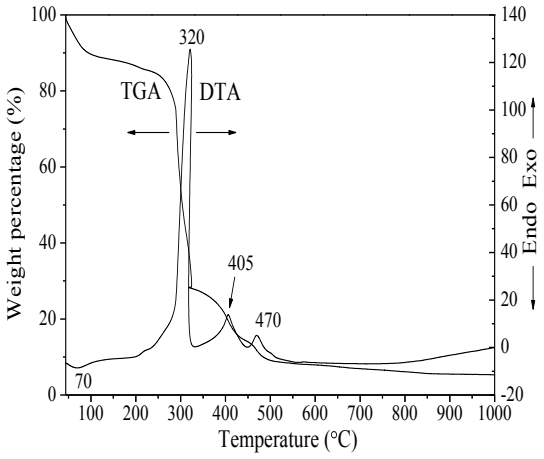

Fig. 1. TG-DTA curves of the $[La(NO_3)_3+ZrOCl_2)]$/PVP composite nanofibers.

3.2 XRD analysis

The composition and phase purity of the samples were examined by XRD, as shown in Fig.2, which displays the XRD patterns of $La_2Zr_2O_7$ annealed at different temperature and $La_2Zr_2O_7$:5%Eu^{3+} annealed at 1150°C for 8 h with the PDF standard card for $La_2Zr_2O_7$(PDF 17-0450). Seen from Fig.2(a), some diffraction peaks appear at 700 °C, which indicate the impurity exist. The main peaks of $La_2Zr_2O_7$ are observed from 900°C. For the $La_2Zr_2O_7$ annealed at 1100 °C or

1150°C, shown in Fig.2(c, d), well-defined diffraction peaks appear, all of which can be indexed to the pyrochlore-structured phase of $La_2Zr_2O_7$ with space group Fd-3m according to the PDF card(No.17-0450). The peak intensity increases at higher heat-treatment temperature, indicating of the enhanced crystallinity [20]. For the Eu^{3+} doped $La_2Zr_2O_7$ calcined at 1150ºC, crystalline $La_2Zr_2O_7$ can be seen from Fig.2e, and all of the diffraction peaks can be readily indexed to those of pure cubic phase with primitive structure of $La_2Zr_2O_7$ (PDF 17-0450). No second phase is detected at these doping levels, indicating that the Eu^{3+} ions can be efficiently built into the $La_2Zr_2O_7$ host lattice by replacing of the La^{3+} ion. The intensity of (222) diffraction peak is the strongest among all of others, suggesting crystal plane (222) growth in a preferred orientation owing to the specific structure.

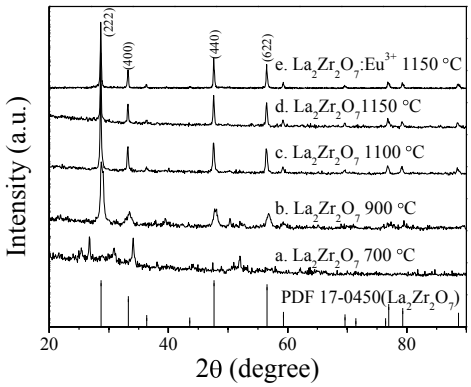

Fig.2 XRD patterns of $La_2Zr_2O_7$ and $La_2Zr_2O_7$:5 mol%Eu^{3+} nanofibers

3.3 SEM and EDX analysis

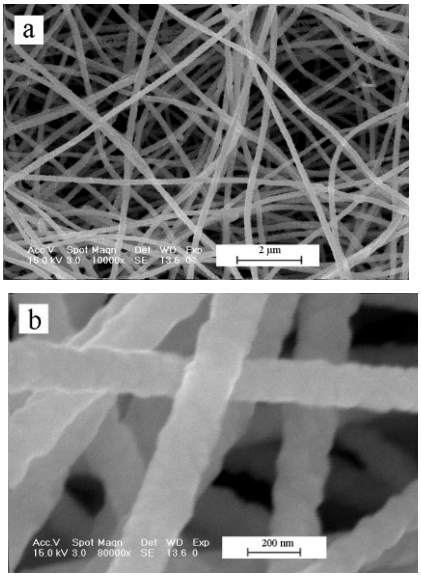

Fig. 3. SEM images of $La_2Zr_2O_7$:5 mol%Eu^{3+} nanofibers annealed at 1150°C with different magnification.

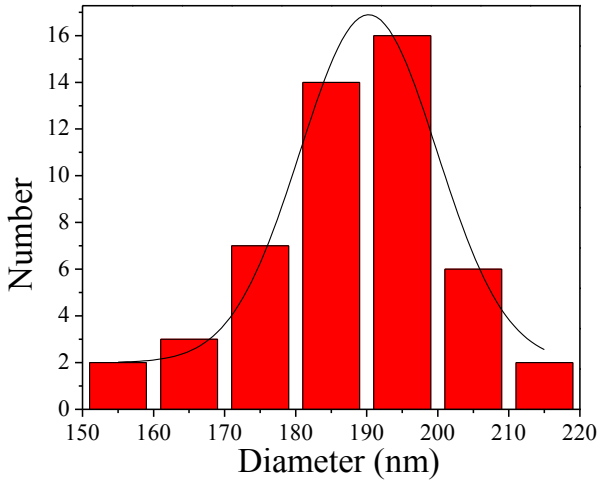

Fig. 4. Distribution histograms of diameters of $La_2Zr_2O_7$:5 mol%Eu^{3+} nanofibers.

Fig. 3(a and b) shows the SEM images of the $La_2Zr_2O_7$:5 mol%Eu^{3+} nanofibers annealed at 1150 °C. Surface of the nanofibers is coarse. They are longer than several millimeters. Average diameter is about 190 nm. The diameter of the nanofibers is not mono-dispersed due to the instability in the course of electrospinning. Fig. 4 shows the histogram of the diameter distribution of $La_2Zr_2O_7$:5 mol%Eu^{3+} nanofibers. The diameters of most nanofibers locate at 180-200 nm.

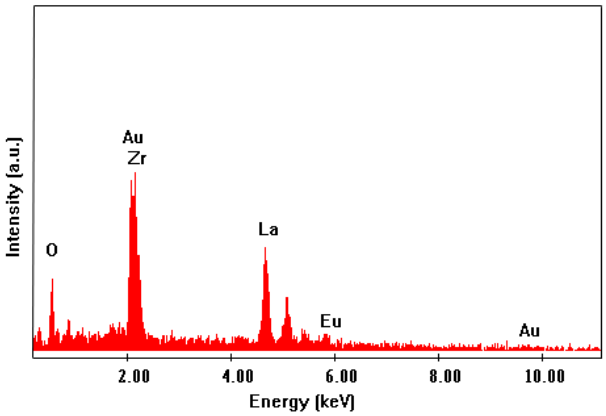

Fig. 5. EDX spectrums of $La_2Zr_2O_7$:5 mol%Eu^{3+} nanofibers.

Fig. 5 shows the EDX spectrum of $La_2Zr_2O_7$:5 mol%Eu^{3+} nanofibers, further confirming that the $La_2Zr_2O_7$:5 mol%Eu^{3+} nanofibers were composed of La, Zr, Eu and O, which was consistent with the XRD result. Inaddition, EDX analysis indicated that the molar ratio of (La+Eu) to Zr was almost 1:1, which was close to the theoretical value.

3.4 Luminescence properties

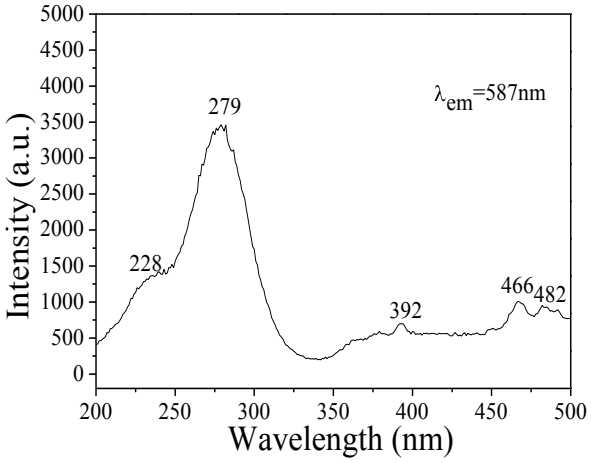

Fig. 6. Excitation spectrum of $La_2Zr_2O_7$:5 mol%Eu^{3+} nanofibers.

Fig. 6 shows the excitation spectra of $La_2Zr_2O_7$:5 mol%Eu^{3+} nanofibers monitored at 587 nm. In the excitation spectra, the strongest peak around 279 nm is associated with the charge transfer(CT) transition of Eu^{3+}-O^{2-}, and the peak around 228 nm is the absorption peak of $La_2Zr_2O_7$ matrix, while the other bands are assigned to the f-f electrons transitions of Eu^{3+}.

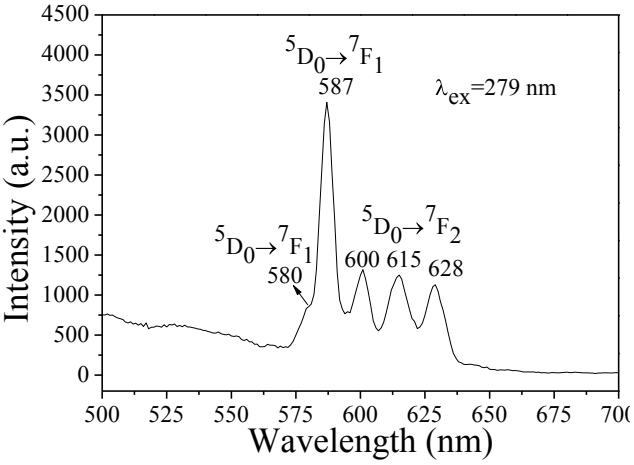

Fig. 7. Emission spectrum of $La_2Zr_2O_7$:5 mol%Eu^{3+} nanofibers (λex=279 nm).

Fig.7 shows the emission spectrum of the $La_2Zr_2O_7$:5 mol%Eu^{3+} nanofibers. Under the excitation of 279 nm, the $La_2Zr_2O_7$:5 mol%Eu^{3+} nanofibers show characteristic emission of Eu^{3+}. The strongest emission peak at 587nm can be assigned to the $^5D_0\rightarrow{}^7F_1$ transitions of Eu^{3+} ions, while the peaks at 580 nm, 600 nm and (612, 627) nm are ascribed to the $^5D_0\rightarrow{}^7F_J$(J = 0, 1, 2) transitions of Eu^{3+} ions, respectively.

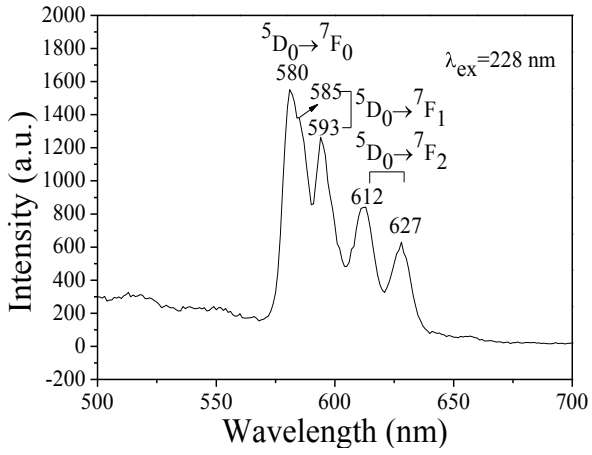

Fig. 8. Emission spectrum of $La_2Zr_2O_7$:5 mol%Eu^{3+} nanofibers (λex=228 nm).

Fig. 8 shows the emission spectrum of the $La_2Zr_2O_7$:5 mol%Eu^{3+} nanofibers under the excitation of 228 nm. The strongest emission peak at 580 nm can be assigned to the $^5D_0\rightarrow{}^7F_0$ transitions of Eu^{3+} ions, while the peaks at (585, 593) nm and (612, 627) nm are ascribed to the $^5D_0\rightarrow{}^7F_J$(J = 1, 2) transitions of Eu^{3+} ions, respectively. When the Eu^{3+} ions would occupy the position with inversion symmetry, the magnetic dipole transition $^5D_0\rightarrow{}^7F_1$ emission peak is expected to have the highest intensity. In addition, $^5D_0\rightarrow{}^7F_0$ is principally believed to be forbidden. Comparing with the intensity of $^5D_0\rightarrow{}^7F_1$ and $^5D_0\rightarrow{}^7F_0$ transitions, it is obvious that the strongest peak varies with different excitation wavelength. It is already know that La^{3+} ions occupy different sites in $La_2Zr_2O_7$ matrix [21-23], and La^{3+} ions are replaced by Eu^{3+} ions in $La_2Zr_2O_7$:5 mol%Eu^{3+} nanofibers. Thus, the way of energy transfer would be changed when excited with different wavelengths because Eu^{3+} ions occupy different sites in $La_2Zr_2O_7$:5 mol%Eu^{3+} nanofibers.

3.5 Formation ,echanism for the $La_2Zr_2O_7$:5 mol%Eu^{3+} nanofiber

The process of electrospinning is so complicated that the formation mechanism for nanofibers via electrospinning remains an open question. On the basis of above analytic results, we propose the formation mechanism for $La_2Zr_2O_7$:Eu^{3+} nanofibers. Rare Earth nitrate, $ZrOCl_2$ and PVP were mixed with DMF to form sol with certain viscosity. PVP acted as template during the formation of $La_2Zr_2O_7$:Eu^{3+} nanofibers. Cations and anions were mixed or absorbed onto PVP to form $[La(NO_3)_3+Eu(NO_3)_3+ZrOCl_2)]$/PVP composite nanofibers under electrospinning. During calcination process, DMF containing in the composite fibers moved to the surface of the fibers, and eventually was evaporated from the composite fibers. With the increase in calcination temperature, PVP, $NO_3^-$and $ZrOCl_2$ were oxidized to volatilize, cations were oxidized into $La_2Zr_2O_7$:Eu^{3+} crystallites, many crystallites were combined into small

nanoparticles, then some small nanoparticles sintered into big nanorods, and these big nanorods were mutually connected to generate $La_2Zr_2O_7:Eu^{3+}$ nanofibers.

4. Conclusions

One-dimensional $La_2Zr_2O_7$: 5 mol%Eu^{3+}nanofibers have been successfully synthesized by means of electrospinning technique in conjunction with sol-gel process. $La_2Zr_2O_7$: 5 mol%Eu^{3+} nanofibers are pyrochlore in structure with space group Fd-3m. The $La_2Zr_2O_7:Eu^{3+}$ nanofibers have coast surface, and average diameter is about 190 nm. The luminescence analysis of the $La_2Zr_2O_7$: 5 mol%Eu^{3+} nanofibers were indicates that under the excitation of 279 nm, 587 nm($^5D_0\rightarrow{}^7F_1$) is the strongest emission peak, when under the excitation of 228 nm, 580 nm($^5D_0\rightarrow{}^7F_0$) is the strongest emission peak.

Acknowledgments

This project is financially supported by NFSC(50972020) and the Science and Technology Development Planning Project of Jilin Province (20040125, 20060504, 20070402), the Scientific Research Planning Project of the Education Department of Jilin Province (2005109, 2006YJT05) and the Scientific Research Project of Environment Protection Bureau of Jilin Province(2006-24).

References

[1] Lin Xu, Hongwei Song, Biao Dong, Yu Wang, Xue Bai, Guolei Wang, Qiong Liu, J. Phys. Chem. C, **113**, 9609 (2009).
[2] Hiyao Hou, Ruitao Chai, Milin Zhang, Cuimiao Zhang, Peng Chong, Zhenhe Xu, Guogang Li, Jun Lin, Langmuir **25**(20), 12340 (2009).
[3] Haiying Wang, Yu Wang, Yang Yang, Xiang Li, Ce Wang, Materials Research Bulletin, **44**, 408 (2009).
[4] Guoping Dong, Yingzhi Chi, Xiudi Xiao, Xiaofeng Liu, Bin Qian, Zhijun Ma, E Wu, Heping Zeng, Danping Chen, Jianrong Qiu, Optics Express, **17**(25), 22514 (2009).
[5] Lili Wang, Zhiyao Hou, Zewei Quan, Chunxia Li, Jun Yang, Hongzhou Lian, Piaoping Yang, Jun Lin, Inorganic chemistry, **48**(14), 6731 (2009).
[6] Yongliang Cheng, Yu Zhao, Yanfei Zhang, Xueqiang Cao, Journal of Colloid and Interface Science **344**, 321 (2010).
[7] Guoping Dong, Xiudi Xiao, Yingzhi Chi, Bin Qian, Xiaofeng Liu, ZhijunMa, E.Wu, Heping Zeng, Danping Chen, Jianrong Qiu, Journal of Materials Chemistry **20**, 1587 (2010).
[8] Chong Peng, Zhiyao Hou, Cuimiao Zhang, Guogang Li, Hongzhou Lian, Ziyong Cheng, Jun Lin, Optics Express **18**(7), 7543 (2010).
[9] Hongwei Song, HongQuan Yu, Guohui Pan, Xue Bai, B.Dong, X. T. Zhang, S. K. Hark, Chem. Mater. **20**, 4762 (2008).
[10] X. Q. Cao, R. Vassenb, D. Stoeve , Journal of the European Ceramic Society **24**(1), 1 (2004).
[11] Aiyu Zhang, Mengkai Lü, Guangjun Zhou, Shumei Wang, Yuanyuan Zhou, Journal of Physics and Chemistry of Solids **67**, 2430 (2006).
[12] Hiroyasu Kido, Sridhar Komarneni, Rustum Roy, Journal of the American Ceramic Society **74**(2), 422 (1991).
[13] Robert Vassen, Xueqiang Cao, Frank Tietz, Debabrata Basu, Detlev Stöver, Journal of the American Ceramic Society **83**(8), 2023 (2000).
[14] K. Koteswara Raoa, Taqveem Banua, M. Vithala, G. Y. S. K. Swamyb, K. Ravi Kumar, Materials Letters **54**(2-3), 205 (2002).
[15] Yoshinori Matsumura, Masaru Yoshinaka, Ken Hirota, Osamu Yamaguchi, Solid State Communications **104**(6), 341 (1997).
[16] J. Nair, P. Nair, E. B. M. Doesburg, J. G. van Ommen, J. R. H. Ross, A. J. Burggraaf, F. Mizukami, Journal of Materials Science **33**(18), 4517 (1998).
[17] Wang Dian-Yuan, Wang Qing-Kai, Chang Zhang-Yong, Guo Yan-Yan,Wu Xing-Hua, Journal of Inorganic Materials **24**(2), 239 (2009).
[18] Cui Qizheng , Dong Xiangting, Wang Jinxian, Mei Li, Journal Of Rare Earths **26**(5), 664 (2008).
[19]Chong Peng, Zhiyao Hou, Cuimiao Zhang, Guogang Li, Hongzhou Lian, Ziyong Cheng, Jun Lin, Optics Express **18**(7), 7543(2010).
[20] Shinobu Fujihara, Kazuaki Tokumo, Chem. Mater. **17**, 5587 (2005).
[21] Henrik Friis, Adrian A. Finch, C. Terry Williams, John M. Hanchar, Phys. Chem. Minerals **37**, 333 (2010).
[22] Chang-Won Lee, Henry O. Everitt, D. S. Lee, A. J. Steckl, J. M. Zavada, Journal of Applied Physics **95**(12), 7717 (2004).
[23] Makoto Ogawa, Yusuke Ide, Masaya Mizushima, Chem. Commun. **46**, 2241 (2010).

*Corresponding author: dongxiangting888@163.com